JOURNAL OF MATERIALS SCIENCE 30 (1995) 2496–2506

The effect of stoichiometry on the stability and a.c. electrical properties of $Li_xNi_{1-y}Co_yO_{2-\delta}$ and $Li_xNi_{1-y}Co_yO_{2-\delta}$–$Al_2O_3$ composites at elevated temperatures

A. OVENSTON*, D. QIN, J. R. WALLS
Department of Chemical Engineering, University of Bradford, West Yorkshire, BD7 1DP, UK

Polycrystalline samples of $Li_xNi_{1-y}Co_yO_{2-\delta}$ ($x = 0.6$, 0.9 and $y = 0.5$, 1, with $\delta \ll 1$ depending on the stoichiometry) with and without the addition of 50 wt% α-Al_2O_3 were prepared and examined by XRD, TGA, DTA and a.c. electrical techniques. Li_xCoO_2 and its mixture with α-Al_2O_3 is unstable above 1050 K. Materials containing Ni were stable up to 1173 K and no interaction with α-Al_2O_3 was found after 6 h at 1173 K. Maximum conductivity in Ar was obtained for $Li_{0.9}Ni_{0.5}Co_{0.5}O_{2-\delta}$ between 100 Hz and 1 MHz up to 950 K. The high temperature conductivity of $Li_{0.9}Ni_{0.5}Co_{0.5}O_{2-\delta}$ could be modified with the addition of α-Al_2O_3 to render it suitable for an RF reactor. At 650 K the conductivity reversibly increased in CO_2 and rapidly decreased in H_2 followed by a slow increase on removal of H_2, behaviour typical of a *p*-type semiconductor. At 870 K the conductivity increased in H_2 due to slow and irreversible reduction of the oxides.

1. Introduction

A novel reactor developed by Walls *et al.* uses radio frequency (RF) power to heat catalysts [1–3]. Heavy hydrocarbons have thus been successfully reformed to useful chemical products without the fouling problems encountered in conventional reactors. The catalyst alone becomes hot, thus gas phase cracking reactions are avoided. Ovenston *et al.* have designed and developed electrically conducting mixed oxide catalysts to specifically suit this type of reactor [2]. Materials of high electronic and/or ionic conductivity are now recognized to have considerable catalytic potential [4–5] and by supplying electromagnetic energy, new mechanisms for activating catalytic reactions may come into play [6]. These catalysts have a number of additional advantages; (a) there is no need for a magnetic component, (b) no need for pre-reduction, (c) they are pre-sintered during preparation and (d) may also contain relatively cheap ingredients. Materials for use at RF must have sufficient magnetic and/or dielectric loss to absorb energy from the electromagnetic field and so reach and maintain reaction temperatures, but without the possibility of thermal runaway occurring [7]. They must also possess the desired catalytic characteristics, i.e. have an active, but selective, long life.

In a recent review, Gellings and Bouwmeester concluded that the conducting properties of ion and mixed conducting oxides have a considerable effect on their catalytic behaviour [5]. a.c. *in-situ* electrical techniques are helpful in trying to relate the complex relationships between catalytic behaviour and electrical properties e.g. for Sn–Sb–O catalysts [8]. Furthermore, the control of the electronic and ionic charge mobilities in ceramics is closely allied to the advances being made in areas such as fuel cell technology, sensors, ceramic membranes, cermets and conducting ceramics. Many of the physical demands such as high strength, stability and conductivity are similar to those required in catalysis.

There are many mixed oxides of high electrical conductivity which may also have potential for use at RF. For example, $Li_xNi_{1-y}Co_yO_2$, investigated by Delmas and Saadoune for use as an anode in solid state lithium batteries, for limited stoichiometry exhibits high mixed (electronic plus ionic) conductivity [9]. These non-stoichiometric materials are mixed conductors having a layered structure through which potassium ions can move with relative ease under an applied d.c. voltage. In this report the a.c. properties of such materials are examined between ambient and 950 K. Samples with $x = 0.6$ and 0.9, for $y = 0.5$ and 1 were prepared, both with and without the addition of alumina to modify the conductivity to desirable levels. The electrical properties were measured between 100 Hz and 1 MHz in an inert argon atmosphere or, in some cases, in reducing and oxidizing atmospheres. The effect of an atmosphere containing mixed H_2 and CO_2 was also studied for two of the composites. Stability is one of the most important characteristics of a catalyst. In this study, differential

* Author to whom correspondence should be addressed.

0022–2461

thermal analysis–thermogravimetric analysis (DTA–TGA) and X-ray diffraction (XRD) methods were used to investigate the stability of these compounds alone and their mixtures with Al_2O_3, particularly after high temperature calcination. The catalytic properties are currently being tested and will be the subject of a further report.

2. Experimental methods

Four $Li_xNi_{1-y}Co_yO_{2-\delta}$ compounds of different stoichiometry with $x = 0.6$ and 0.9 each for $y = 0.5$ and 1 were prepared by fusion of Li_2CO_3, NiO and Co_3O_4 in stoichiometric proportions by firing for two hours at 773 K followed by 48 h under O_2 at 1273 K [9]. Half of each material was finely ground and intimately mixed with 50 wt % α-Al_2O_3. Pellets 1.2 cm diameter and about 4 mm thick were made using 10 kg force for about 5 min. The list of materials and codes subsequently used in the text are shown in Table I.

Pt enamel contacts were fired on to the ends of the pellets for 1 h at 1073 K. The samples were predried at 400 K to eliminate any moisture until the electrical properties became stable. Tests were then performed at pre-set temperatures between 300 and 950 K using a Eurotherm gold reflecting furnace and Hewlett Packard 4194A impedance analyser using the methods described in detail elsewhere [10]. Care was taken to compensate for the effects of the leads, particularly at high temperatures for the samples with very low impedance [11].

To account for small variations in the depths (d) of the pellets, all the conductance data has been normalized (assuming $G \propto 1/d$) to $d = 4$ mm. The relative magnitudes of the effective conductivities may then be directly compared for each sample. For conductivity ($\propto G$) measurements the sample was represented by a capacitance (C_p) in parallel with a resistance ($= 1/G$). The real and imaginary components of the dielectric constant are proportional to C_p and G/ω respectively, where ω is the angular frequency. The loss tangent, a property independent of geometry and useful for comparison with other materials, is given by $G/(\omega C_p)$. For complex impedance plots the samples were represented by a resistance (R) in series with a reactance (X); 200 data points between 100 Hz and 1 MHz were used [10].

Except where stated, experiments were conducted in Ar flowing at 10 ml min^{-1}. When used, the flow rates of CO_2 and H_2 were mixed with Ar and controlled using Brookes flow meters; part of the outlet gas stream was directed to a VG quadrapole mass spectrometer for analysis and the remains of the gaseous products were burnt off.

On-line computer-controlled Shimadzu DTA-50 and Shimadzu TGA-50 equipment were used for DTA and TGA. Experiments were conducted on powdered samples using a platinum crucible in a N_2 atmosphere at a flow rate of 30 ml min^{-1}. A temperature range of 293–1173 K with a rate of increase of 30 K min^{-1}. was employed. XRD measurements were carried out using a Siemens Diffractometer 5000 with CuK_α radiation at room temperature.

TABLE I Composition and coding of materials

NC1	$Li_{0.6}Ni_{0.5}Co_{0.5}O_{2-\delta}$	NC2	$Li_{0.6}Ni_{0.5}Co_{0.5}O_{2-\delta}$ + α-Al_2O_3
NC3	$Li_{0.6}CoO_{2-\delta}$	NC4	$Li_{0.6}CoO_{2-\delta}$ + α-Al_2O_3
NC5	$Li_{0.9}Ni_{0.5}Co_{0.5}O_{2-\delta}$	NC6	$Li_{0.9}Ni_{0.5}Co_{0.5}O_{2-\delta}$ + α-Al_2O_3
NC7	$Li_{0.9}CoO_{2-\delta}$	NC8	$Li_{0.9}CoO_{2-\delta}$ + α-Al_2O_3

3. Results

3.1. Stability

XRD spectra of Li–Ni–Co–O ceramics alone, e.g. NC1, NC3 and NC5, are shown in Fig. 1 with the Miller indices of the Bragg peaks marked beside the respective peaks. The crystal patterns are similar to that of $LiCoO_2$ reported elsewhere [12]. Thus the structural framework of $LiCoO_2$, which is indexed to the trigonal space group R3m, is retained for all samples. The d spacing with hkl data (Miller indices) for NC1, NC3 and NC5 are recorded in Table II. The Miller index is for $LiCoO_2$ according to Zhecheva and Stoyanova [12].

The peaks for $Li_{0.6}CoO_2$ (NC3) are the same as reported for $LiCoO_2$, except that two impurity peaks at $d = 2.834$ and $d = 2.417$ appear and arise from cobalt oxides. Peaks for $Li_xNi_{0.5}Co_{0.5}O_2$, $x = 0.6$, 0.9 (NC1 and NC5) also show a similar character to those of NC3. This indicates that the substitution of Ni for 50 at% Co in the crystal does not result in a change in the structural framework. Additional peaks for NC1 ($d = 2.056$) and for NC5 ($d = 2.072$) to the peaks for NC3 were observed which are due to the contribution of some NiO impurity in the sample. The amount of Li exhibits little effect on the structural framework whether or not Ni is substituted for some of the Co, but a small shift in the peaks is observed as shown in Table II.

The mixtures of α-Al_2O_3 and Li–Ni–Co–O ceramics NC2, NC4 and NC6 were also analysed by XRD. No additional peaks other than those for α-Al_2O_3 and the respective Li–Ni–Co–O material were observed. Thus no new species were formed and hence no interaction between α-Al_2O_3 and Ni–Co compounds had occurred. Fig. 2 shows the XRD spectrum for NC6 which was calcined in N_2 flowing at 30 ml min^{-1} for 6 h at 1173 K. The spectrum clearly shows the peaks for α-Al_2O_3 and NC5 alone without the addition of further peaks.

DTA-TGA characteristics for NC1, NC3 and NC5 are shown in Fig. 3. Both NC1 and NC5 show no thermal peak and weight loss within the recorded temperature range and are therefore stable up to 1173 K. The shifts of the base-line in the DTA curves are caused by the change of heat capacity of the samples as temperature rises. NC3 is stable up to 1050 K, however, an endothermic peak appears between 1050 K and 1130 K with a peak at 1093 K. A weight loss of 1.6% of the total sample weight was also recorded for NC3 at 1113 K. NC7 ($Li_{0.9}CoO_{2-\delta}$), with the same Co/O ratio as NC3 but with a larger Li content, shows an endothermic peak at 1093 K and a weight loss at 1113 K. Zhecheva and Stoyanova [12] also observed the endothermic peak and a weight

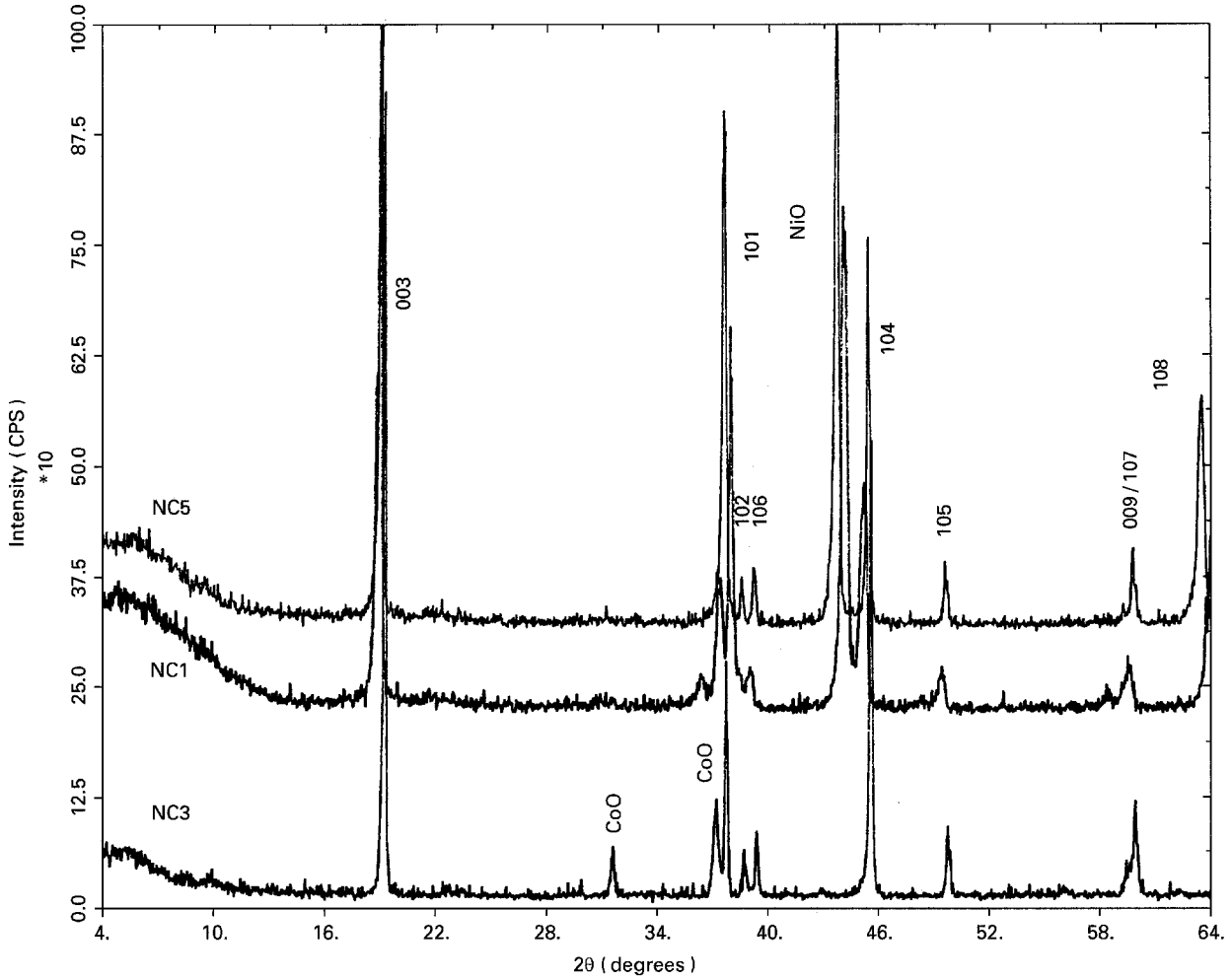

Figure 1 XRD spectra of NC1, NC3 and NC5 with the Miller indices of the Bragg peaks marked.

TABLE II Crystallographic data, *d* spacing and *hkl*

hkl	NC1	NC3	NC5
003	4.666	4.606	4.654
101	2.372	2.385	2.393
102	2.310	2.326	2.335
006	2.306	2.287	2.297
104	2.008	1.992	1.999
105	1.845	1.833	1.839
009	1.547	1.544	1.548

loss for $Li_{1-x-y}H_yCoO_2$ and suggested that a framework reconstruction and a release of O_2 occurred at this temperature. The temperature for release of O_2 may be higher than the thermal peak due to diffusion of O_2 from the bulk of the crystal.

The DTA-TGA characteristics for NC2, NC4 and NC6 were also examined. DTA (Fig. 4) shows NC2 and NC6 to be as stable as NC1 and NC5 but NC4 shows an endothermic peak at 1093 K similar to that observed for NC3. Thus the behaviour of the samples containing α-Al_2O_3, NC2, NC4 and NC6, is similar to that of NC1, NC3 and NC5, respectively. The TGA spectra for NC2, NC4 and NC6 also show the same trends. Thus, α-Al_2O_3 has no interaction with the Li–Ni–Co–O ceramics and no effect on the stability of the composites within the experimental conditions.

3.2. Electrical characteristics in Argon

Figs 5 and 6 show the effect of temperature and frequency on conductance for samples of $Li_{0.6}Ni_{0.5}Co_{0.5}O_{2-\delta}$ alone and with the addition of α-Al_2O_3 (NC1 and NC2). The characteristics are typical of materials showing both dipole relaxation losses and conduction from hopping charge carriers at high temperatures. At lower temperatures, frequency has a large effect with the power n in $\sigma \propto \omega^n$ of order 0.8 near 1 MHz, a value typical of predominantly dipole effects arising from structural defects and impurities in the material [10]. In contrast, at the higher temperatures, frequency has little effect, but the conduction of the charge carriers becomes thermally activated, with an activation energy of about 1.1 eV at 100 Hz.

At the lower temperatures, due to dipole losses arising from both components in the composite material, the addition of the insulator has little effect on the characteristics (Fig. 6). However, as the temperature is increased to 950 K the conductance is reduced by an order of magnitude due to the reduction in the total concentration of charge carriers which largely emanate from the $Li_{0.6}Ni_{0.5}Co_{0.5}O_{2-\delta}$ component. The activation energy is unaltered. Thus alumina may be added to the conductor in order to modify the overall conductivity of the composite at high temperatures but it will not significantly alter the conduction properties at low temperatures.

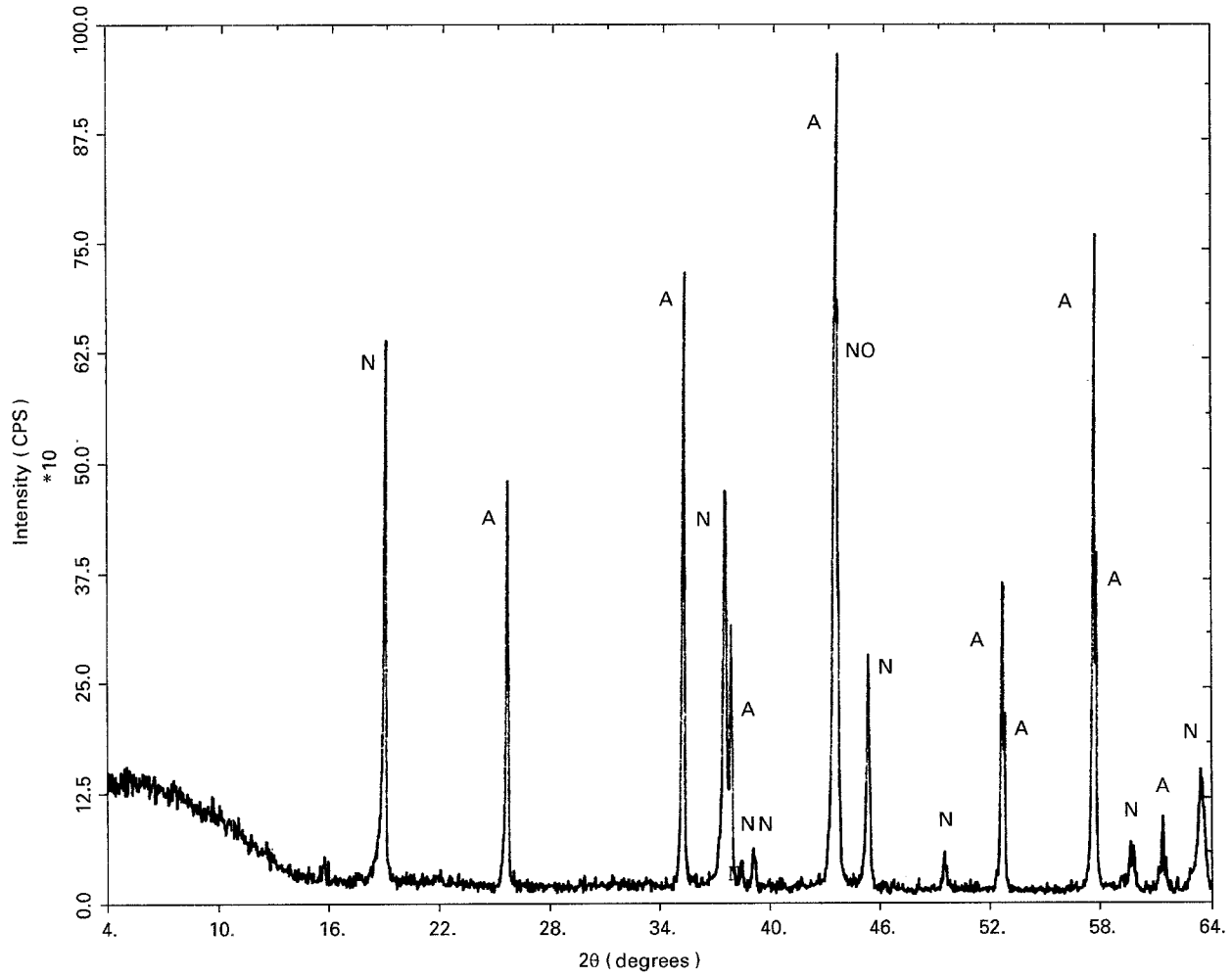

Figure 2 XRD spectrum of NC6 which was calcined in N_2 for 6 h at 1173 K. A: Al_2O_3, NO: NiO, N: $Li_{0.9}Ni_{0.5}Co_{0.5}O_{2-\delta}$.

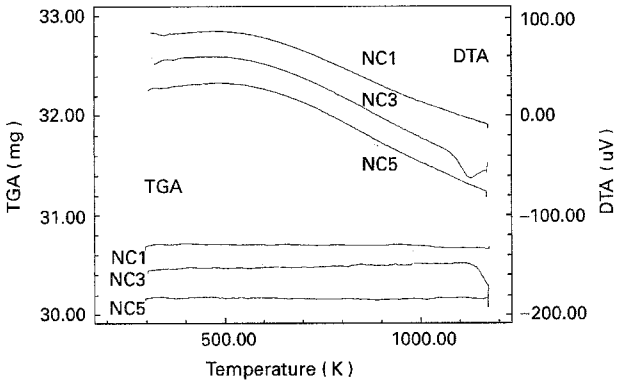

Figure 3 DTA-TGA spectra for NC1, NC3 and NC5.

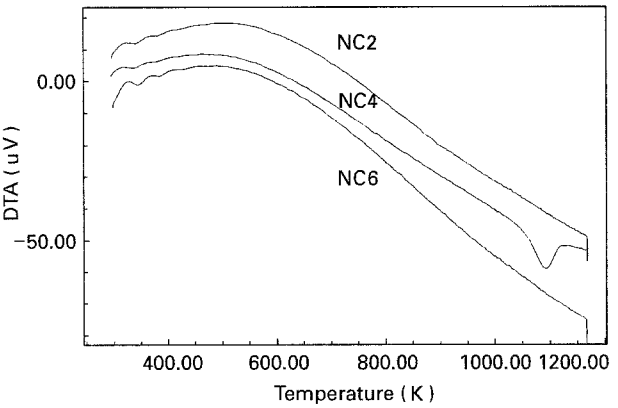

Figure 4 DTA spectra of NC2, NC4 and NC6.

Previous work has shown that the behaviour at 1 MHz can reasonably be extrapolated to 20 MHz (the operating frequency of the RF reactor), thus data at 1 MHz can give a good indication of the potential of the material to heat up in such a reactor. The effect of the stoichiometry of the $Li_xNi_{1-y}Co_yO_{2-\delta}$ component on the electrical characteristics at 1 MHz is shown in Fig. 7. A substantial difference between the pure materials is shown, with the conductance decreasing in the order NC5 > NC3 > NC1 > NC7. Thus $Li_{0.9}Ni_{0.5}Co_{0.5}O_{2-\delta}$ exhibits the highest conductance whilst sample NC1 with a reduced Li content showed a similar temperature dependence but conductances of lower magnitude. In contrast, samples without Ni (NC3 and NC7), were more conducting for the least Li content except at the highest temperatures. Here, a high activation energy approaching 3.7 eV, typical of ionic conduction, was observed. This complex behaviour may be associated with the relative sizes of the Ni and Co ions, the resulting ease with which the alkali ions can move between the layered structure and the number of sites available for these ions to move into, (for further details see section 4). For the high alkali content, comparison between samples NC5 and NC7 shows

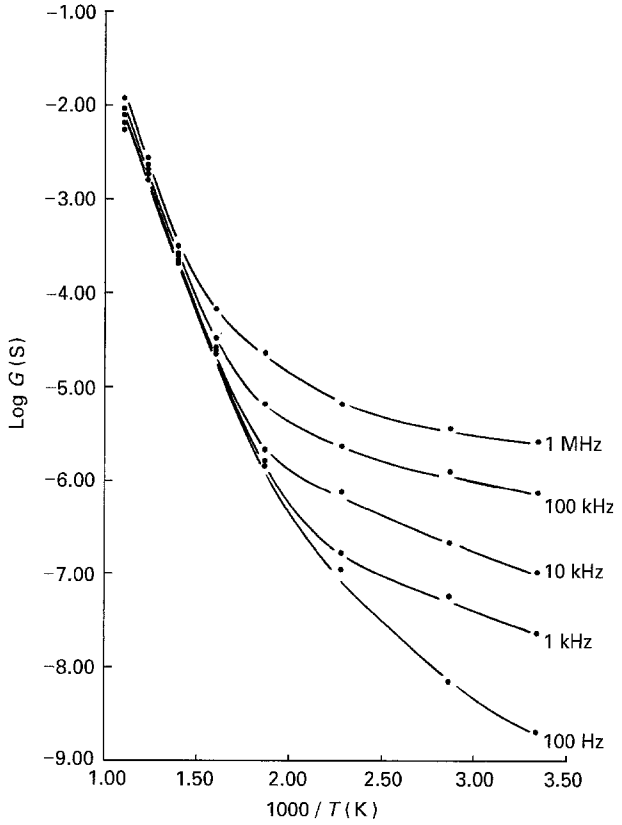

Figure 5 Conductance–temperature–frequency characteristics for NC1 in argon.

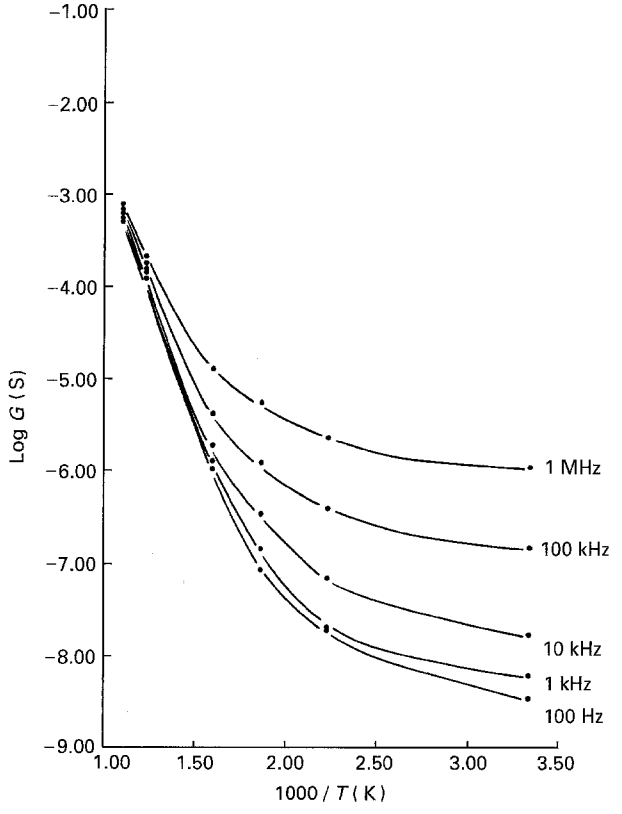

Figure 6 Conductance–temperature–frequency characteristics for NC2 in argon.

the presence of Ni to have a large and beneficial effect on the conductivity. However, for a lower Li content, the effect of Ni is reversed. Thus relationships between the amount of Li and the substitution of Ni for 50 at % of the Co in the lattice is complex.

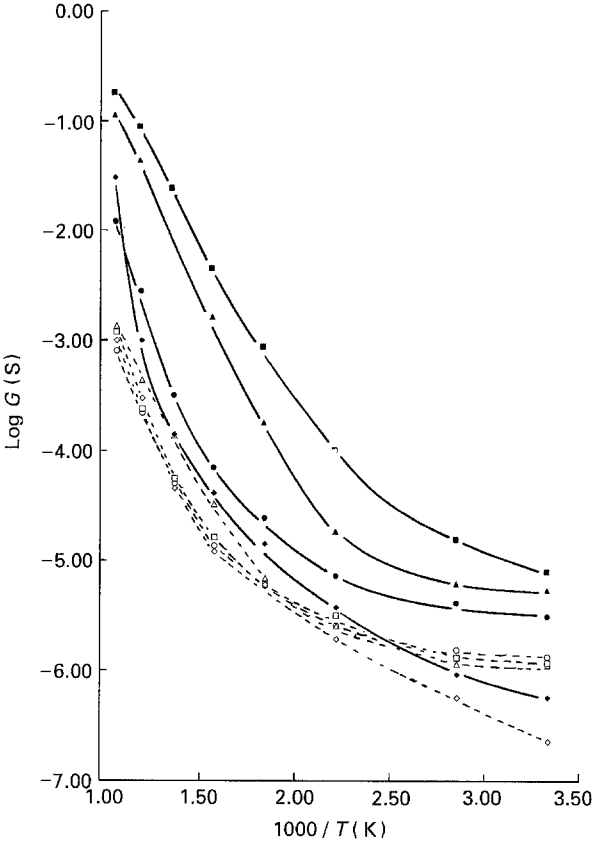

Figure 7 Comparison of conductance–temperature characteristics at 1 MHz in argon for NC1 (●), NC2 (○), NC3 (▲), NC4 (△), NC5 (■), NC6 (□), NC7 (◆) and NC8 (◇).

With the addition of alumina, the characteristics were less varied, with similar magnitudes for the conductances and activation energies of about 0.84 eV between 700 and 950 K. At temperatures approaching 300 K, temperature had almost no effect, except for sample NC8 (Fig. 7). These results signify that the contribution of mobile charge carriers to the conductance at 1 MHz is greatly reduced by the alumina particles. Alumina is able to reduce the overall conductance at high temperatures by 1 or 2 orders of magnitude, but has much less effect at the lower temperatures.

Values of the loss tangent (tan δ) at 1 MHz, shown in Table III, show NC5 to have the highest loss at all temperatures. Near room temperature, tan δ decreases in the order NC5 > NC6 > NC7 > NC3 > NC1 > NC8 > NC2 > NC4 with values between 0.45 to 0.043. These low values are typical of a dielectric response governed by dipole relaxation from dipoles arising from imperfections and impurities in the structure of the material. The alumina effectively dilutes such losses. At higher temperatures, e.g. 800 K, tan δ exceeds unity and ranges from 1.7 to 24, values typical of dielectric losses from free rather than bound thermally activated charges. At this temperature the loss tangent decreases in the order NC5 > NC3 > NC1 > NC7 > NC8 > NC4 > NC2 > NC6.

Since both free and bound charges have time to travel further during a half cycle at low frequencies, it is useful to study the conductance characteristics at the lowest frequency of 100 Hz. Fig. 8 shows NC5 to again have a substantially higher conductivity than all

TABLE III Loss tangent at 1 MHz

Temperature	NC1	NC2	NC3	NC4	NC5	NC6	NC7	NC8
300 K	0.15	0.064	0.2	0.043	0.45	0.4	0.35	0.13
800 K	6.0	1.7	22.0	2.7	24.0	1.6	4.0	3.6

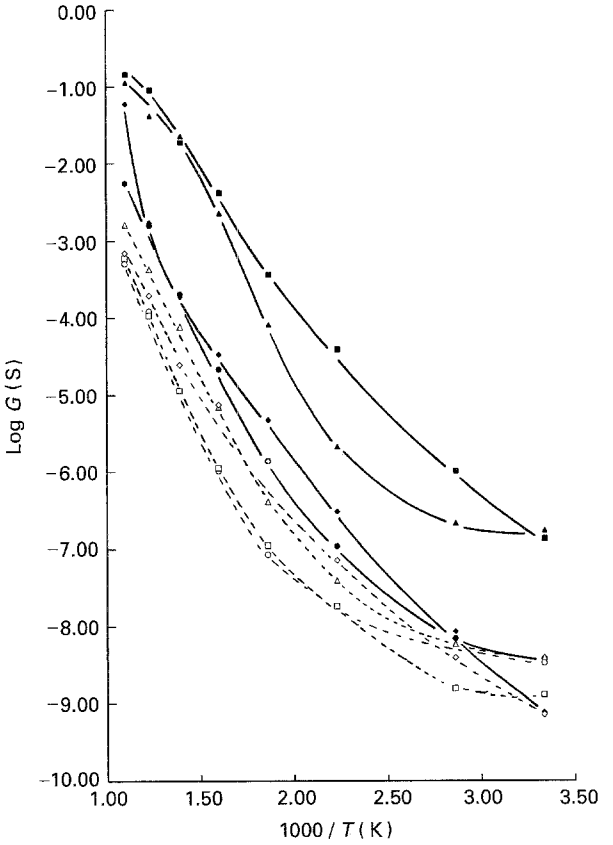

Figure 8 Comparison of conductance–temperature characteristics at 100 Hz in argon for NC1 (●), NC2 (○), NC3 (▲), NC4 (△), NC5 (■), NC6 (□), NC7 (◆) and NC8 (◇).

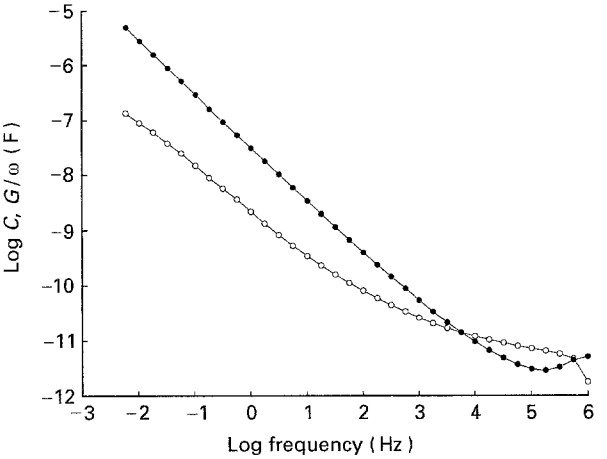

Figure 9 Dielectric dispersion ($C \propto \varepsilon'$ (○) and $G/\omega \propto \varepsilon''$(●)) for NC5 at room temperature in air.

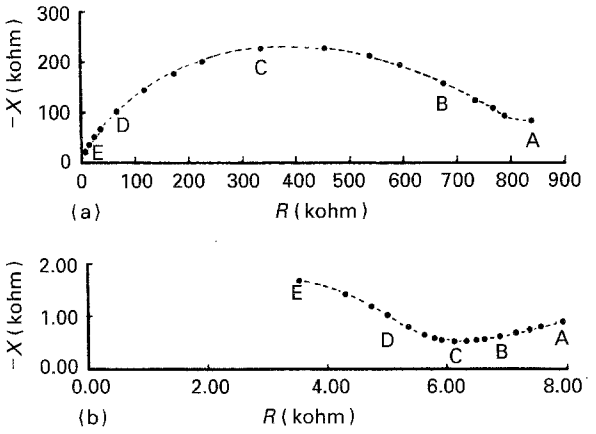

Figure 10 Complex impedance diagrams for NC2 at (a) 628 K and (b) 819 K showing frequency points at 100 Hz, A; 1 kHz, B; 10 kHz, C; 100 kHz, D; and 1 MHz, E.

other samples, whilst all samples show activated behaviour to prevail even at temperatures approaching ambient. For example, NC7 has an activation energy of about 0.52 eV near 300 K. Composites containing alumina showed more dependence on the stoichiometry of the conducting component than at 1 MHz and all samples showed an activation energy of about 1.1 eV at high temperatures. The general effect of the insulator was to decrease the magnitude of the conductance above ambient temperatures. For the most lossy material (NC5) the addition of alumina (NC6) effectively reduced the conductance by up to three orders of magnitude depending on the temperature.

Measurements of a fresh sample of NC5 in air over a wider range of frequency between 5.6×10^{-3} Hz and 1 MHz showed that the behaviour above 100 Hz could be extrapolated to the lower frequencies. Fig. 9 shows the dielectric dispersion at room temperature, with the dielectric constant, $\varepsilon' \propto C$ and the loss factor, $\varepsilon'' \propto G/\omega$. The data is typical of materials exhibiting low frequency dispersion associated with thermally activated charge carriers, with a well defined power law for the conductivity (σ) with $\sigma \propto \omega^n$ where $n = 0.04$, i.e. negligible frequency dependence up to about 1 kHz [13].

Complex impedance diagrams were also examined for some samples and all showed a single or partial semicircle at lower temperatures with a large angle of tilt of about 23° to the real axis, e.g. Fig. 10. This is typical for materials of mixed or principally electronic conductivity [10]. No evidence for overlapping semicircles was seen between 100 Hz and 1 MHz, hence separate loss processes relating to bulk or grain boundary phenomena could not be distinguished. As temperature increased a low frequency spur was observed, which became increasingly dominant as temperature increased further. This spur is usually seen when ionic conduction becomes significant [10]. For samples showing the highest conductivities, the effect of frequency is so small that such diagrams are meaningless.

3.3. Effect of atmosphere

3.3.1. $Li_{0.6}CoO_{2-\delta}$

The effects of CO_2 (10 ml min^{-1}) and H_2 (10 ml min^{-1}) diluted by Ar (50 ml min^{-1}) on a composite without Ni, $Li_{0.6}CoO_{2-\delta} + Al_2O_3$ (NC4), were studied at 650 K and 870 K. The conductances varied in a similar fashion at each frequency but the proportional changes were lower at 1 MHz as shown in Figs 11 and 12. At 650 K, CO_2 caused a small reversible increase in the conductance, whilst H_2 caused a rapid large decrease which was not immediately reversed on removal of the gas. However on re-examination a week later (day 2, Fig. 11(b)) the conductance had regained its initial value in Ar. After a second exposure to H_2, the conductance tended to increase slowly with time. The almost immediate response to both gases indicates surface chemisorption; for H_2, the strongly bound gas is desorbed much more slowly than for CO_2. The capacitance was found to vary in the same way as the conductance.

At the higher temperature of 870 K, the effect of CO_2 was similar but the response to H_2 was quite different, as shown in Fig. 12. For the latter, the conductance decreased initially but then rapidly increased. On passing a mixture of these gases over the sample the conductance continued to increase with the frequency dependence of the conductance becoming negligible. At high temperatures it is probable that the cobalt oxide component will be reduced to metallic Co. The behaviour is typical of a porous semimetallic type of material. On cooling, the conductance remained at a high level and independent of frequency as expected for metallic rather than semiconducting behaviour. The material was reoxidized in air at 650 K

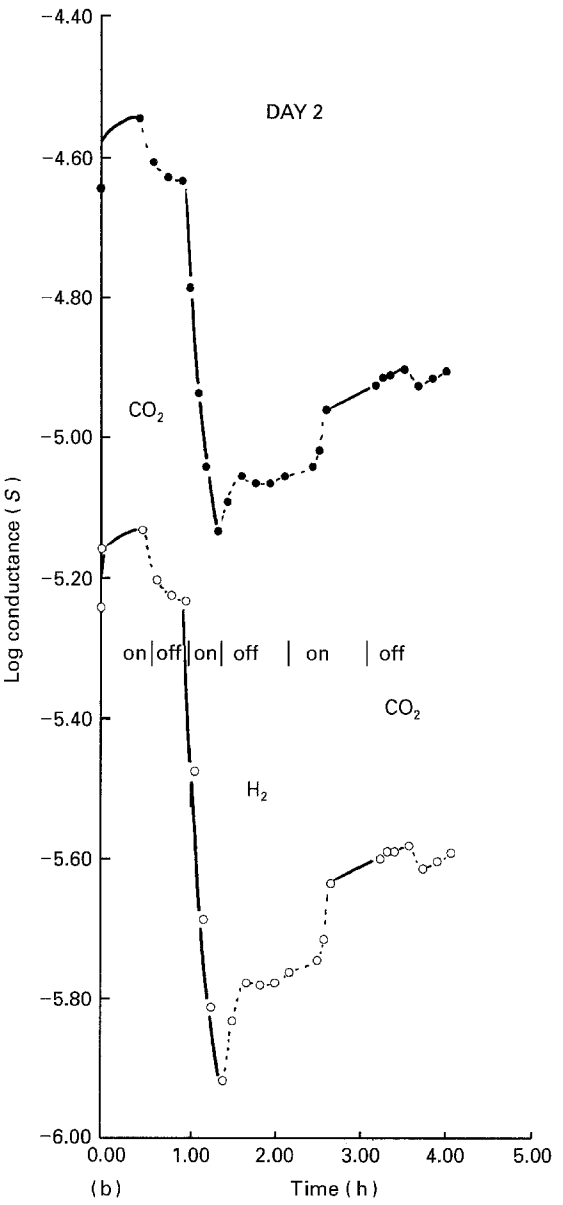

Figure 11 Effect of CO_2 and H_2 on the conductance of NC4 at 650 K at 100 Hz (○) and 1 MHz (●) for (a) day 1 and (b) day 2.

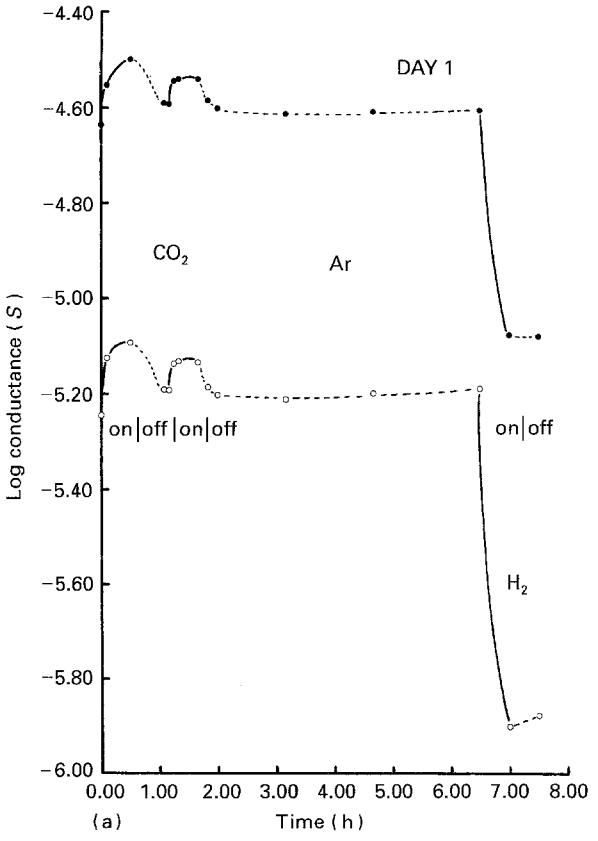

for 3 h to test whether or not the original state could be established. Although the conductance at this temperature was reduced by an order of magnitude, the lower temperature values remained high, the values showing activated behaviour with a low activation energy of about 0.15 eV. Thus it was not possible to reoxidize this composite back to its original state. Since permanent changes had taken place, this particular material was not considered for further investigation.

3.3.2. $Li_{0.9}Ni_{0.5}Co_{0.5}O_{2-\delta}$

The effect of atmosphere on the more stable compound NC6 containing $Li_{0.9}Ni_{0.5}Co_{0.5}O_{2-\delta}$ and alumina was found to be similar to NC4 but less pronounced at 640 K, as shown in Fig. 13. For the gas mixture $H_2 + CO_2$ diluted by Ar, there is an initial decrease followed by a less rapid increase in conductance, (Fig. 13). The complex change in conductance may be partly due to the production of some steam and CO from the reverse Water Gas Shift reaction

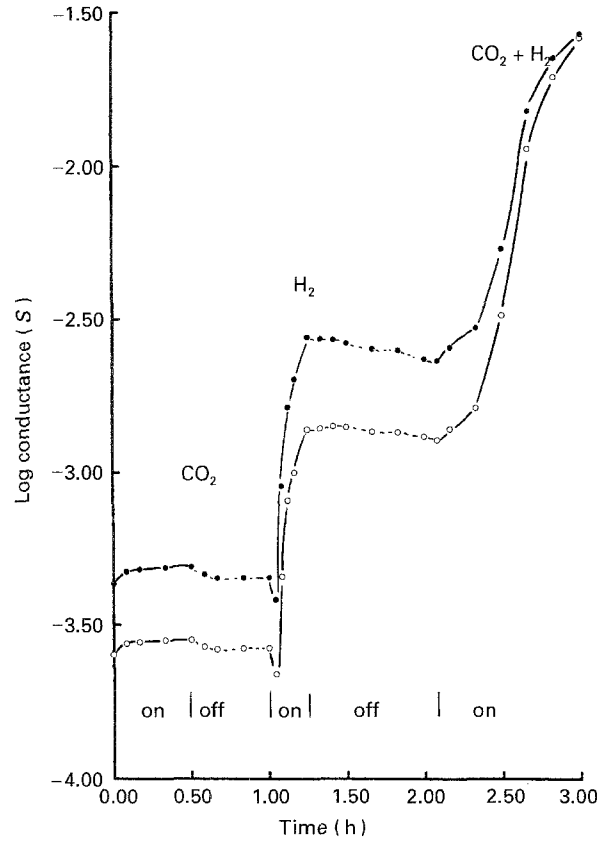

Figure 12 Effect of CO_2 and H_2 on the conductance of NC4 at 870 K at 100 Hz (○) and 1 MHz (●).

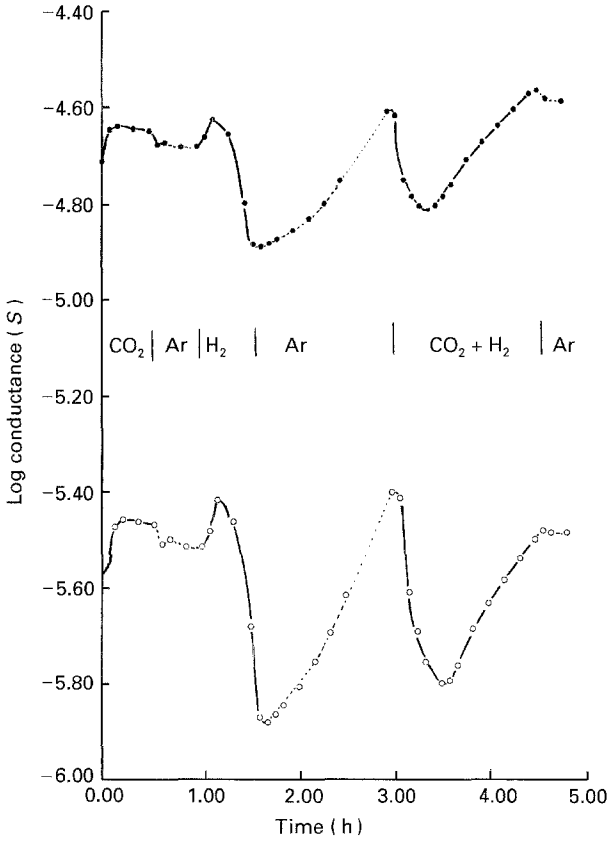

Figure 13 Effect of CO_2 and H_2 on the conductance of NC6 at 640 K at 100 Hz (○) and 1 MHz (●).

($CO_2 + H_2 \Leftrightarrow CO + H_2O$). No irreversible changes occurred at this temperature. At 738 K, a small steady increase in conductance was observed in the $H_2 + CO_2$ atmosphere. At the higher temperature of

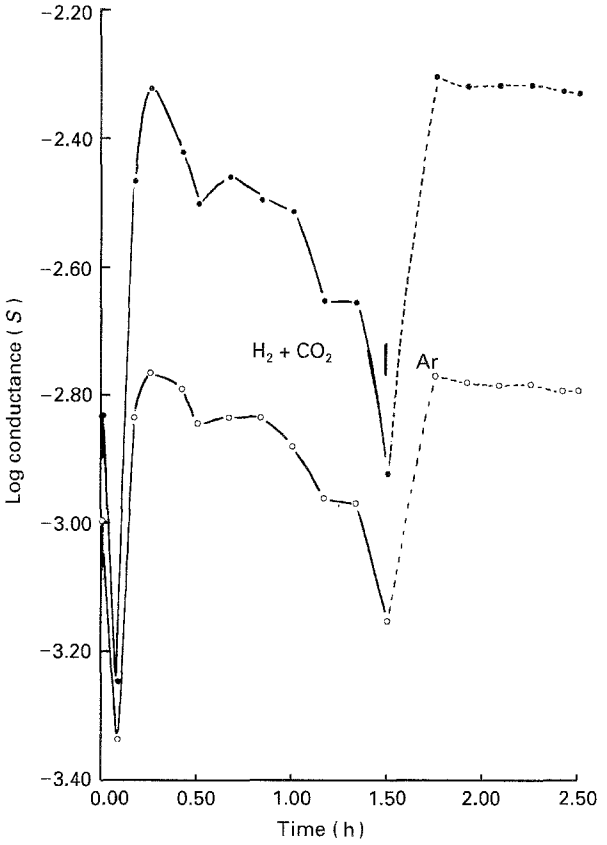

Figure 14 Effect of CO_2 and H_2 on the conductance of NC6 at 838 K at 100 Hz (○) and 1 MHz (●).

838 K, the effect of these gases caused only relatively small changes in the electrical properties, (Fig. 14) in comparison with the less stable material without Ni (Fig. 12). For the $Li_{0.9}Ni_{0.5}Co_{0.5}O_{2-\delta}$ composite, exposure to an $H_2 + CO_2$ atmosphere for 1.5 h resulted in an increase in conductance at 1 MHz by a factor of about 8, whilst a further exposure for 1.5 h caused a further three-fold increase. The G-f-T characteristics were not substantially altered by the above gaseous treatments apart from an effective increase in conductance by about one order of magnitude at all temperatures and frequencies. These changes are not large enough to cause problems of thermal runaway in an RF reactor and further work is underway to test the catalytic activity and selectivity of this material.

4. Discussion

4.1. Stability

As discussed in section 3.1, Li–Ni–Co–O ceramics retain the structural framework of $LiCoO_2$. This can be described as a close-face-centred-cubic packing of oxygen ions, where the octahedral sites are alternately occupied by Li^+ and CO^{3+}, making up alternate (1 1 1) layers of Li–O and Co–O [9, 12, 14]. It is an α-$NaFeO_2$ type crystal structure. Evidence from XRD indicates that the substitution of Ni for Co does not change the structural framework of $LiCoO_2$. This fact suggests that Ni will occupy the same octahedral sites as Co. The arrangement of Ni and Co may be random, but in order to obtain electrical neutrality, Co^{2+} and Co^{3+} are the preferred oxidation states in most cobalt oxides although Co^{4+} has also been found in

Li–Ni–Co–O ceramics [9, 12]. Ni^{2+} is the preferred oxidation state in most nickel oxides. Although little evidence about the oxidation state of Ni in Li–Ni–Co–O ceramics has been reported, a $Ni^{2+\delta}$ ($\delta > 0$) is expected in order to obtain an electronic balance. The ionic diameter of Ni^{2+} (69 pm, 1 pm = 10^{-12} m) is larger than that of Co^{3+} (63 pm) [15]. The increase of the content of Co in Li–Ni–Co–O ceramics evidently reduces the lattice parameters a and c [9]. This fact confirms that the ionic diameter of Ni is larger than that of Co. To occupy a crystal site an ion should not have too large or too small a diameter in comparison with the host ion which it replaces. If the diameter is too large, the crystal would not be stable; if it is too small, the crystal would be metastable and the crystal type would revert to a more stable one under certain conditions. NC3 ($Li_{0.6}CoO_{2-\delta}$) is stable at lower temperatures but unstable at higher temperatures. The reason may be that the ionic diameter of Co is too small for the structure, the structure will transform to a stable one; the spinel Co_3O_4 has been suggested [12]. An internal reduction–oxidation reaction occurs during the transformation. The process can be represented by the chemical equation

$$12Li_{0.6}Co^{3+}O_{1.8} \Rightarrow 4Co_3O_4 + O_2 + 3.6\ (Li_2O) \quad (1)$$

The oxidation state Co^{3+} has been used in $Li_{0.6}CoO_2$ in order to conserve the electronic and mass balances. The release of O_2 is then 2.9% of the total weight which is larger than the observed value of 1.6%. The diffusion of O_2 from the crystal bulk may result in a reduction of the observed value and a higher temperature is required for the total transformation. The substitution of Ni for Co expands the crystal of $LiCoO_2$ and stabilizes the structure due to its larger ionic diameter.

Some of the Li in the structure may be easily removed or exchanged with other ions and hence result in non-stoichiometric proportions of the alkali component [9, 12, 14]. The Li content will affect the volume of the lattice cell and the conductance but not the structural framework. It shows little effect on the stability of the crystal in the laboratory conditions used. The further investigation of the function of Li and its ion-exchanged products may be of benefit to the improvement of catalytic and other properties. α-Al_2O_3 is a well known catalyst support and widely used; the investigation of XRD and DTA-TGA suggests that there is no interaction between α-Al_2O_3 and Li–Ni–Co–O ceramics in the range of temperature used in the experiments. Therefore, it is possible to add α-Al_2O_3 to Li–Ni–Co–O ceramics in order to adjust their conductance to levels suitable to the RF reactor whilst maintaining the crystal structure and other properties of the catalyst.

4.2. a.c. characteristics

For some reactions involving hydrocarbons it is believed that catalysts having both high electronic conductivity and a high ionic conductivity are beneficial [4]. The Li–Ni–Co–O conducting ceramics fall into this category. Furthermore Ni itself is a widely used catalyst with well characterized catalytic properties, Co is often included as a catalytic component to help deter sintering problems, and Li has more recently been used when coupled to MgO in the studies of catalysts with effective activity and selectivity for the oxidative coupling of methane [16]. For semiconductors, low band gap materials generally lead to greater activity, some complex oxides are more active and selective than simple oxides [17].

Layered materials $Li_xNi_{1-y}Co_yO_{2-\delta}$ showed that for $y \geqslant 0.4$, Co^{4+} ions appear, leading to a p-type electronic conductivity [9]. As the amount of alkali ion increases, near $x \to 1$, the ionic conductivity decreases rapidly as the number of available sites for Li^+ ion diffusion becomes very small. This behaviour could result from the presence of larger Ni ions in the interlayer space for Ni rich phases. Thus these materials are mixed conductors dependent on the stoichiometry and the complex inter-relation between x and y. The simultaneous presence of Ni atoms in the layer and of a statistical Li^+ ion distribution in the interlayer space leads to an electronic localization. For $x = 0.9$ (NC5), the high conductivity observed is due to superposition of a Ni–O–Ni electronic hopping conduction [9].

Delmas and Saadoune also found for a high cobalt material that as the amount of Li increased, the electronic d.c. conductivity at room temperature decreased. Thus at room temperature, for 100 Hz, NC3 would be expected to have a greater conductivity than NC7 as was observed (Fig. 8). However, in the a.c. measurements reported here, the ionic conductivity of the alkali ions is included in the overall conductance measured and the relative contributions of electronic and ionic diffusion cannot be assessed. If samples having the same Ni/Co ratio are compared, i.e. NC1 and NC5, the highest conductance is associated with the larger amount of Li. If samples with the same amount of Li are compared, e.g. NC5 and NC7, the conductivity is much higher for the material containing Ni. Since the Ni ions are larger than the Co ions, the presence of the Ni may obstruct any diffusion of Li ions. In the absence of Ni, at high temperatures, the conductivity starts to rise rapidly for $Li_{0.9}CoO_{2-\delta}$ as the Li ions become more mobile (NC7 in Fig. 7).

4.3. Effect of atmosphere

At low frequencies, particularly at high temperatures, the frequency dependence of the conductivity becomes negligible (i.e. in $\sigma \propto \omega^n$, $n \to 0$), indicating that thermally activated charge carriers dominate the a.c. behaviour [13]. For NC4 and NC6, the increase in conductance in CO_2 and decrease in H_2 are typical behaviour for a p-type semiconductor, for which holes are the principal charge carriers. The power index n tended to increase in both CO_2 and H_2 indicating that additional surface dipoles are formed. These will be subject to relaxation losses in an a.c. field which will increase as frequency increases, hence the conductivity

rises slightly more with increasing frequency in these atmospheres. At the higher frequencies approaching 1 MHz, $n \simeq 0.3$ and increase in H_2 indicating that the lattice is becoming more regular in a reducing atmosphere.

4.4. RF reactor

For possible use as a catalyst in a packed bed reactor heated by RF power it is necessary that the conductivity at the frequency concerned is sufficiently high at room temperature for the material to heat up from ambient and that the conductivity is sufficiently high at the desired temperature of reaction for the material to reach that temperature [7]. However, it is important that the high temperature conductivity and the activation energy are not too high or the heat absorbed will always exceed the heat losses and thermal runaway will occur if the control of the input power to the reactor is insufficiently fast. This phenomenon has been observed with other highly conducting materials but may be controlled by the addition of suitable proportions of an insulator [7]. Comparison with other materials shows NC5 to have too high a conductivity at 950 K, but NC6 to have a sufficiently high conductivity at this temperature and just have a sufficiently high conductivity at low temperature for the material to absorb heat from cold. The proportion of alumina could be adjusted to suit the particular reactor. For use in an RF fluidized bed reactor, where the surface area per unit volume of the particles is significantly higher, the heat losses will be greater thus a higher conductivity could be tolerated and the need for an insulating component may no longer be necessary.

5. Conclusions

Polycrystalline samples of the layered mixed conductors $Li_xNi_{1-y}Co_yO_{2-\delta}$ ($x = 0.6, 0.9$ and $y = 0.5, 1$) prepared both with and without the addition of 50 wt % alumina were electrically examined in an Ar atmosphere. They all exhibited dielectric dispersion typical of lossy solid dielectrics in accordance with the universal theory of dielectric response. At high temperatures approaching 950 K, thermally activated charges carriers dominated the a.c. conduction processes between 100 Hz and 1 MHz, while nearer 300 K, relaxation losses in dipoles arising from impurities and imperfections in the lattice predominated. Here the effect of temperature is reduced, whilst the effect of frequency is pronounced with $\sigma \propto \omega^n$ with n about 0.7. Complex impedance diagrams showed tilted semicircles inclined at about 23° to the real axis at lower temperatures, typical of mixed or predominantly electronic conductors, with a low frequency spur appearing at higher temperatures usually associated with ionic conductivity [10]. It was not possible to distinguish between bulk, grain boundary and surface conduction processes from these diagrams.

The effect of stoichiometry was complex, with critical relationships between the amount of Li and the amount of Ni, which cannot be fully understood without further investigation. Without Ni present the activation energies at high temperatures are high and reflect significant alkali ion diffusion. $Li_{0.6}CoO_{2-\delta}$ and its mixture with α-Al_2O_3 is unstable above 1050 K. The substitution of Ni for Co stabilizes the crystal structure, but Li has little effect on the stability of the crystal. No interaction was observed between α-Al_2O_3 and Ni–Co compounds even after calcination at 1173 K for 6 h.

The greatest conductivity was shown for $Li_{0.9}Ni_{0.5}Co_{0.5}O_{2-\delta}$ for which the loss tangent was also a maximum e.g. 24.0 at 800 K. This material was stable up to 1173 K in an inert atmosphere and showed no reaction with alumina after 6 h at 1173 K. Although Ni is apparently needed to achieve stability it reduces the ionic conductivity due to reducing the gap between the crystalline layers [9]. For some stoichiometries too much Li can leave too few vacancies for the ions to move into; hence the amount of alkali is probably critical and needs further attention. The addition of alumina is needed in order to reduce the net RF conductivity and eliminate the possibility of thermal runaway at high temperatures. Although alumina can reduce the conductance by several orders of magnitude at high temperatures, at lower temperatures it has much less effect and consequently will have little effect on the rate of heating from ambient. For use in a new fluidized bed reactor, heat losses are relatively greater and the addition of an insulator may prove unnecessary.

In an oxidizing atmosphere these materials are stable, however, in a reducing environment reduction to metallic Co and Ni may occur at high temperatures. Changes in chemisorption, both reversible and irreversible can be correlated with changes in conduction and other electrical properties. Weber *et al.* in a recent review of the opportunities in highly conducting electroceramics emphasized that the conduction mechanisms and associated activation energies in highly doped systems need to be better understood [18]. This reports contributes to the understanding of the AC conduction properties of conducting Li–Ni–Co–O ceramics between ambient and elevated temperatures approaching 1000 K. Future work will explore the potential of such materials for use as catalysts in a variety of reactors heated by electromagnetic energy.

Acknowledgements

Len Shields is thanked for his helpful comments, Niala Choudhry for preparing the samples, Dan Sprînceană for assisting with the electrical measurements and Terry Ramdeen (Kings College Dielectrics Group) and John Pugh (Dielectric Instrumentation) for making measurements at low frequencies. The SERC are gratefully thanked for their contributions to the equipment.

References

1. J. R. WALLS, J. K. LEE and A. OVENSTON, in Proceedings of the Eighth International Symposium on Chemical Reactor Engineering Edinburgh, vol. **87** (Institute of Chemical Engineers, Pergamon Press, 1984) p. 463.

2. A. OVENSTON, S. MIRI and J. R. WALLS, in "Advanced ceramics in chemical processing engineering", edited by B. C. H. Steele and D. P. Thompson, Ser. Brit. Ceram. Proc. **43** 57 (Institute of Ceramics, London, 1989).
3. M. T. MIRZA, J. R. WALLS and S. A. A. JAYAWEERA, *Thermochimica Acta* **152** (1989) 203.
4. A. W. SLEIGHT, *Science* **208** (1980) 895.
5. P. J. GELLINGS and H. J. M. BOUWMEESTER, *Catal. Today* **12** (1992) 1.
6. A. OVENSTON, J. R. WALLS, A. ALLEN and W. ARMSTRONG, *J. Mater. Sci.* **29** (1994) 1358.
7. A. OVENSTON and J. R. WALLS, *Trans. I. Chem. E.* **68** (1990) 530.
8. A. OVENSTON, D. SPRÎNCEANÃ, J. R. WALLS and M. CÃLDÃRARU, *J. Mater. Sci.* **29** (1994) 4946.
9. C. DELMAS and I. SAADOUNE, *Solid State Ionics* **53–56** (1992) 370.
10. A. OVENSTON and J. R. WALLS, *J. Catal.* **140** (1993) 464.
11. Hewlett-Packard 4194A Gain Phase/Impedance Analyser manual (1985)
12. E. ZHECHEVA and R. STOYANOVA, *J. Solid State Chem.* **109** (1994) 47.
13. R. M. HILL and A. K. JONSCHER, *Contemp. Phys.* **24** (1983) 75.
14. K. MIZUSHIMA, P. C. JONES, P. J. WISEMAN and J. B. GOODENOUGH, *Mat. Res. Bull.* **15** (1980) 783.
15. J. A. Dean (ed.), "Lange's Handbook of Chemistry" 13th edition (McGraw-Hill Book Company, New York, 1985).
16. J. H. LUNSFORD, *Catal. Today* **6** (1990) 235.
17. O. V. KRYLOV, *ibid.* **18** (1993) 209.
18. W. J. WEBER, H. L. TULLER, T. O. MASON and A. N. CORMACK, *Mat. Sci. Eng.* **B18** (1993) 52.

Received 22 August
and accepted 10 October 1994